Flood Susceptibility Mapping of Greater Hyderabad Municipal Corporation Region of Telangana State, India: A Multi Criteria Approach using GIS and AHP

Reddy Lokanath M.[1*], Reddy Madhusudhan M.[2], Reddy Venkata Rami Y.[3], Harshada K.[4] and Reddy Vishnu Vardhan L.[5]

1. Department of Civil Engineering, G. Pullaiah College of Engineering and Technology, Kurnool, Andhra Pradesh, INDIA
2. Department of Civil Engineering, Institute of Aeronautical Engineering, Dundigal, Hyderabad, Telangana, INDIA
3. Department of Civil Engineering, SVR Engineering College, Nandyal, Andhra Pradesh, INDIA
4. Department of Civil Engineering, Malla Reddy Engineering College, Medchal, Hyderabad, INDIA
5. Department of Civil Engineering, University College of Engineering JNTUK, Narasaraopet, INDIA

*lokanathreddygpcet@gmail.com

Abstract

This manuscript presents a comprehensive study on flood susceptibility mapping in the Greater Hyderabad Municipal Corporation (GHMC) region of Telangana State, India, utilizing Geographic Information Systems (GIS) and the Analytic Hierarchy Process (AHP) as a multi-criteria approach. The primary objective of this research is to develop a robust flood susceptibility mapping framework for GHMC, considering various thematic maps including distance to river, elevation, flow accumulation, flow direction, drainage density, contour, Landsat 8, normalized difference vegetation index (NDVI), land use and land cover (LULC), annual rainfall, roughness, slope, stream network, topographic wetness index (TWI) and flood susceptibility map. Through the integration of these thematic maps, we have successfully delineated areas prone to flooding within the GHMC region.

The study highlights the importance of utilizing multiple criteria and GIS techniques for accurate flood susceptibility assessment. The results indicate that areas with high drainage density, low elevation and proximity to rivers are more susceptible to flooding. Moreover, factors such as land cover, rainfall intensity and terrain roughness significantly influence flood susceptibility. Conclusions drawn from this study emphasize the significance of incorporating spatial analysis and decision-making techniques in flood risk management and urban planning initiatives.

Keywords: Flood susceptibility mapping, Geographic Information Systems, Analytic Hierarchy Process, GHMC, GIS-AHP Multi-criteria approach and Urban flood risk management.

Introduction

Hyderabad, the capital city of Telangana State, India, stands as a vibrant metropolis with a rich historical and cultural heritage. Renowned for its economic significance, technological advancements and diverse population, Hyderabad serves as a pivotal center of commerce, education and administration in the region. However, amidst its urban sprawl and rapid development, the city grapples with recurring challenges posed by natural disasters, particularly floods. The history of Hyderabad and its surrounding regions, under the purview of the Greater Hyderabad Municipal Corporation (GHMC), bears witness to various instances of flooding. Hyderabad, the bustling capital city of Telangana State, India, has long been entrenched in a narrative that intertwines progress with challenges posed by the forces of nature. This is especially evident in the city's recurring encounters with devastating floods, which have left indelible scars on its landscape and collective memory.

The most notables in recent history are the catastrophic floods of 2020, which unleashed unprecedented fury upon Hyderabad and its environs[66]. The 2020 Hyderabad floods, triggered by Deep Depression, unleashed havoc across the city in October 2020[70]. Characterized by torrential downpours and flash flooding, this calamity wreaked havoc in various neighbourhoods including Balapur, L. B. Nagar and parts of the Old City such as Hafiz Baba Nagar and Al Jubail colony[18]. The deluge, exacerbated by overflowing reservoirs and rivers, resulted in significant loss of life and property, underscoring the vulnerability of Hyderabad to the vagaries of nature.

However, the story of flooding in Hyderabad is not confined to recent events alone. The city's tumultuous relationship with floods dates back centuries, with historical accounts documenting catastrophic inundations that have left lasting scars on its landscape and populace. The Great Musi Flood of 1908 stands as a stark testament to the city's vulnerability, claiming tens of thousands of lives and causing widespread devastation along the banks of the Musi river[19].

The resilience of Hyderabad's inhabitants in the face of such adversity is exemplified by tales of survival amidst the deluge. From the heroic efforts of those who sought refuge atop a 200-year-old tamarind tree within Osmania Hospital to the poignant verses penned by Urdu poet Amjad Hyderabadi in the aftermath of personal tragedy, the city's narrative is one of both resilience and remembrance[73]. Against this backdrop of historical precedent and

*** Author for Correspondence**

contemporary challenges, this study seeks to delve into the dynamics of flood susceptibility in Hyderabad and the GHMC region. By harnessing the power of Geographic Information Systems (GIS) and the Analytic Hierarchy Process (AHP), we endeavour to unravel the complex interplay of environmental factors and urban dynamics that contribute to flood risk[4,5,8,14]. Through our research, we aim to offer insights that not only enhance our understanding of flood susceptibility but also inform proactive strategies for disaster mitigation and urban resilience in Hyderabad and beyond.

Background

Hyderabad, as the capital city of Telangana State, occupies a pivotal position in India's socio-economic landscape. Renowned for its rich history, cultural diversity and rapid urbanization, Hyderabad serves as a hub of innovation, commerce and governance in the region. However, the city's meteoric rise has been accompanied by a host of challenges, chief among them being the recurrent threat of flooding[20,23].

Floods in Hyderabad pose significant risks to lives, infrastructure and livelihoods, underscoring the urgent need for robust flood risk management strategies[43]. The city's topography, characterized by low-lying areas and proximity to rivers, exacerbates its vulnerability to inundation during heavy rainfall events[27,72]. Furthermore, rapid urbanization and inadequate infrastructure exacerbate the impacts of floods, leaving communities vulnerable to displacement, economic losses and public health crises. Considering these challenges, understanding and mitigating flood risk in the GHMC assumes paramount importance. A comprehensive understanding of flood susceptibility, informed by scientific methodologies and spatial analysis, is essential for effective disaster preparedness and response[12,36].

Objectives of the Study

1. To delineate areas within the GHMC region that are most susceptible to flooding based on various thematic maps.
2. To develop a robust flood susceptibility mapping framework for the GHMC region using GIS and the AHP as a multi-criteria approach.

Review of Literature

The literature review provides valuable insights into flood susceptibility mapping techniques and highlights previous studies conducted in the field, shedding light on the methodologies employed and key findings. Flood susceptibility mapping techniques encompass a range of approaches including statistical models, remote sensing and GIS, which are utilized to assess the likelihood of areas experiencing flooding based on various factors such as topography, land use and hydrological characteristics[29].

Previous studies in flood susceptibility mapping have explored diverse geographic regions and urban contexts, offering valuable lessons and best practices for flood risk assessment and management[44-50]. By synthesizing the existing body of literature, this review sets the stage for the current study, providing a foundation for the methodology and analysis conducted herein.

Flood Susceptibility Mapping Techniques: Liuzzo et al[39] conducted a study comparing different methods for flood susceptibility mapping using GIS. They analysed four methodologies: frequency ratio, frequency ratio combined with logistic regression, frequency ratio combined with Shannon's entropy index and statistical index. These methods were applied to Devon County, Southwest England, considering ten conditioning factors. The statistical index model showed the highest accuracy in predicting flood susceptibility, with elevation, slope and stream distance identified as significant factors[52].

The study suggests that flood susceptibility maps can aid in water resource and land use planning and management, with potential for further research on including additional conditioning factors like vegetation density[65].

Pham et al[49] proposed and validated three ensemble models based on Best First Decision Tree (BFDT) and ensemble learning techniques for flood susceptibility prediction in Nghe Province, Vietnam. They utilized 10 flood influencing factors and 126 historical flood events to train and validate the models. The decorate-BFT ensemble model outperformed bagging-BFT and random subspace-BFT models, achieving an area under the receiver operating characteristic curve value of 0.989. These ensemble models demonstrated superior prediction capabilities compared to single BFT models, suggesting their utility in flood early warning systems and mitigation planning. Further research could explore their applicability to different regions and types of floods or natural hazards.

Mudashiru et al[44] reviewed flood hazard analysis methods, emphasizing multi-criteria decision-making (MCDM), statistical and machine learning (ML) techniques. They highlighted the importance of accurate flood hazard/susceptibility mapping for effective flood risk management. MCDM methods integrate stakeholder input with less complexity, while statistical methods address uncertainty and provide spatial flood maps. ML methods offer fast and reliable flood mapping but may have limitations. The study suggests addressing challenges through evaluation, ensemble modelling and data quality improvement for better flood management decisions[44].

Arabameri et al[2] studied flood hazard susceptibility mapping (FHSM) in the Kiasar watershed, Iran, using four methods: evidential belief function (EBF), frequency ratio (FR), TOPSIS and VIKOR. They compared statistical and multi-criteria decision-making (MCDM) approaches using area under receiver operating characteristic curve. EBF showed the best prediction rate (0.987) and success rate (0.946) followed by FR, TOPSIS and VIKOR. Slope, distance to stream and land use were identified as key factors in flood

occurrence. The study recommends combining statistical and MCDM methods for accurate FHSM in similar areas.
Seydi et al[61] developed a Cascade Forest Model (CFM) for flood susceptibility mapping, utilizing satellite imagery and field data to identify flood-inundated areas. The CFM outperformed six other machine learning methods, achieving over 95% overall accuracy and 0.95 area under the receiver operating characteristic curve in two study areas. Flood-prone regions in the Karun and Gorganrud basins were identified, with CFM demonstrating superior accuracy and generalization capabilities compared to other models. The study suggests that future research should focus on optimizing model hyperparameters automatically.

Critical review on Flood Susceptibility Mapping studies using GIS-AHP Approach: Vilasan et al[74] utilized remote sensing, GIS and AHP and fuzzy-analytical hierarchy process methods to create flood susceptibility maps for Ernakulam district, Kerala. Factors like slope, soil types, land use and stream density were considered. The maps were validated with satisfactory area under the receiver operating characteristic curve values, indicating good prediction capability. The study highlights anthropogenic activities and natural factors contributing to floods and provides valuable information for land-use planning and policymaking to mitigate future flood risks[67].

Kotecha et al[30] emphasized the increasing frequency of extreme hydrological events like floods due to climate change and urbanization. They focused on flash floods, which pose significant risks to property and lives. Using GIS, remote sensing and spatial AHP, they identified flood-prone areas in Rajasthan's Luni basin, highlighting tehsils with high susceptibility. This study aims to mitigate flash flood risks in the Western region of Rajasthan through effective flood hazard mapping and management strategies.

Study Area

Telangana, India's newest state, is situated at 17.8° N 79.18° E on the southern-central part of the Indian peninsula[26]. Positioned on the elevated Deccan Plateau, it is the eleventh-largest State in India, covering an area of 1,12,077 square kilometres. According to the 2011 census, Telangana is the 12th most populous State with a population of 3,51,93,978 residents[9]. The Telangana State was officially formed on June 2, 2014, separating from Andhra Pradesh and its designated capital city is Hyderabad. Hyderabad, the capital of Telangana, encompasses the twin cities of Hyderabad and Secunderabad.

This vibrant metropolis, boasting an urban population of around 6 million, has a history dating back 400 years and was once the seat of the wealthy Nizams of Hyderabad. Located on the banks of the Musi river, Hyderabad is surrounded by unique prehistoric rock formations resembling petrified gray elephants. The district's geographical coordinates range between 77° 30' E and 79° 30' E longitude and between 16° 30' N and 18° 20' N latitude. According to the 2011 census, the district's population is 39,43,323 constituting 11.20% of the State's total population, with a 2.97% decadal growth rate[9]. Figure 1 illustrates the geographical location map of the GHMC boundary in Telangana.

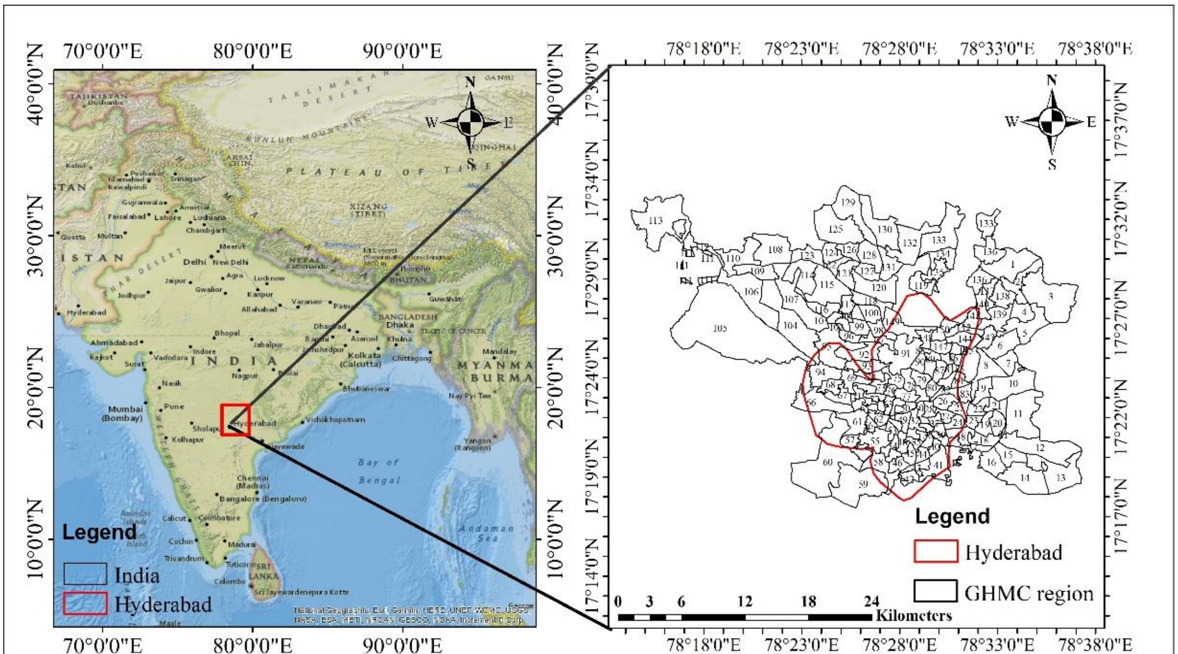

Fig. 1: Geographical location of GHMC boundary from India.

Material and Methods

Utilizing data acquired from the USGS website, specifically Landsat 8 imagery and historical rainfall data gathered from the IMD website, a comprehensive methodology was employed to generate a detailed flood susceptibility map for the region[64,67]. The process involved integrating various thematic maps derived from GIS analysis, incorporating factors such as elevation, slope, roughness, contours and aspect, along with additional variables like land use land cover, flow accumulation, stream direction, stream network, drainage density, flow length, distance from the river, soil composition, NDVI and TWI[46].

To initiate the process, Landsat 8 imagery was utilized to extract essential terrain features such as elevation, slope and aspect. This data, combined with information on roughness and contours, provided a comprehensive understanding of the region's topography and terrain characteristics[76]. Furthermore, factors influencing hydrological processes, such as land use land cover and soil type, were incorporated into the analysis to assess their impact on water flow and infiltration. NDVI was employed to gauge vegetation density, which plays a crucial role in mitigating soil erosion and regulating water absorption[6]. In addition, hydrological parameters including flow accumulation, stream direction, stream network, drainage density and flow length were analysed to delineate water pathways and to identify areas prone to flooding[13,15]. Moreover, proximity to water bodies, represented by distance from the river, was considered a significant factor in assessing flood susceptibility.

The culmination of these analyses facilitated the generation of a flood susceptibility map, utilizing a combination of the AHP-derived weights and GIS-based overlay techniques[21,25]. This approach allowed for a comprehensive evaluation of various factors contributing to flood vulnerability, providing stakeholders with valuable insights into potential flood-prone areas[28]. The step-by-step methodology employed in this study is illustrated in figure 2.

Data collection and processing

Data acquisition is a critical initial step in the preparation of flood susceptibility maps which play a vital role in disaster management and urban planning[31-35]. Leveraging advanced geospatial technologies such as GIS facilitates a comprehensive approach to data gathering and analysis. The data collection process commenced with the retrieval of pertinent geospatial datasets from authoritative sources[37]. Landsat-8 satellite imagery and Shuttle Radar Topography Mission Digital Elevation Model (SRTM-DEM) data were obtained from the United States Geological Survey (USGS) website[10,23]. These datasets provide invaluable insights into land cover, topography and terrain characteristics essential for flood susceptibility assessment[69].

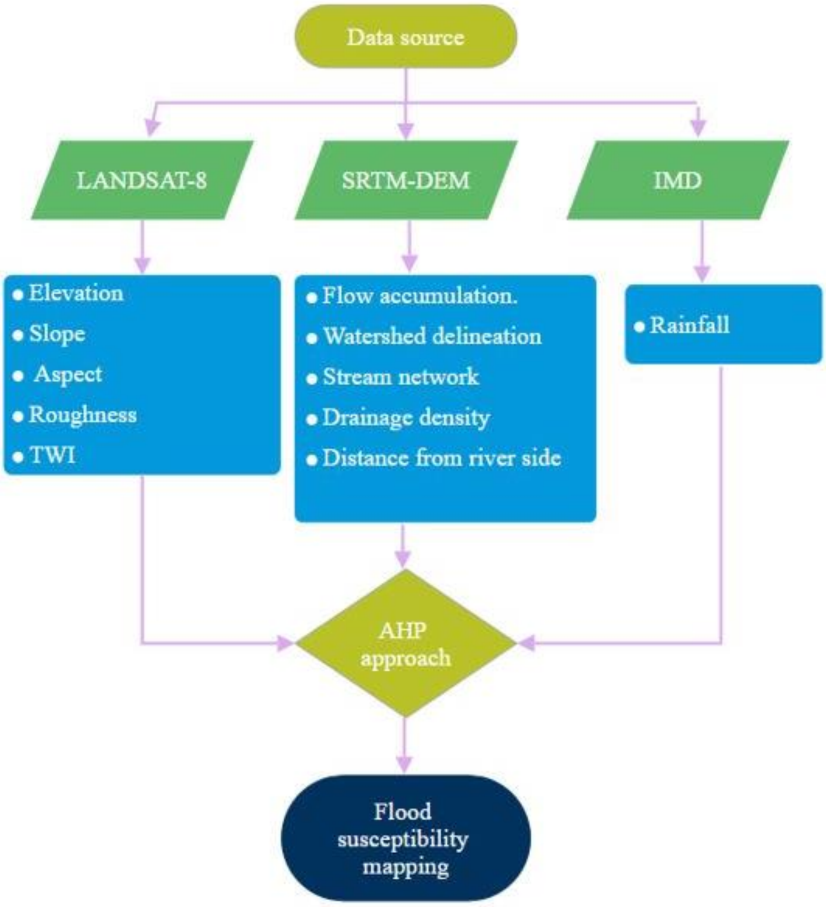

Fig. 2: Methodology adopted in this study to prepare a flood susceptibility map of GHMC.

To augment this information, historical rainfall data spanning previous years were procured from the Indian Meteorological Department (IMD) website. Precipitation patterns over time serve as crucial indicators for understanding flood risk and vulnerability[41]. Subsequently, the collected data underwent meticulous processing utilizing advanced GIS techniques. Various thematic maps were generated, each offering distinct insights into factors influencing flood susceptibility. GIS procedures involved in data processing encompassed as:

- **Aspect Analysis:** Determining the direction of slope faces, influencing water runoff patterns.
- **Distance to River Calculation**: Assessing proximity to water bodies, a significant determinant of flood risk.
- **Drainage Density Mapping:** Identifying areas with high concentration of streams and rivers, indicative of flood-prone regions.
- **Elevation Modelling:** Analyzing terrain elevation to identify low-lying areas susceptible to inundation.
- **Flow Accumulation and Flow Direction Analysis:** Understanding water flow pathways to predict flood propagation.
- **Calculation of Topographic Wetness Index (TWI):** Quantifying terrain wetness to assess flood susceptibility[3].
- **Generation of Thematic Maps:** Including NDVI, roughness, slope and stream network, providing additional insights into environmental factors affecting flood vulnerability[3].
- **Integration of Landsat-8 Imagery:** Incorporating satellite imagery for land cover classification and change detection, aiding in flood susceptibility assessment[11].
- **Flood Susceptibility Mapping:** To generate comprehensive flood susceptibility maps, employ weight overlay techniques by scaling all previously developed thematic maps on a scale of 1 to 5, considering their respective significance in flood susceptibility[42]. Combine these scaled thematic maps to create integrated maps that provide a holistic view of flood-prone areas.

Results and Discussion

The colour infrared map (using bands 3, 4 and 5 respectively) and elevation map within the GHMC region are pivotal datasets crucial for the groundwork of flood susceptibility mapping in the area[48]. Offering detailed insights into land cover patterns, vegetation distribution and urban infrastructure, the colour infrared map aids in comprehending surface characteristics and potential flood pathways[24,63].

Simultaneously, the elevation map, categorized into 5 distinct elevation classes ranging from the lowest to the highest elevation of 255 meters, furnishes indispensable data concerning terrain fluctuations and areas prone to inundation during flood occurrences[51].

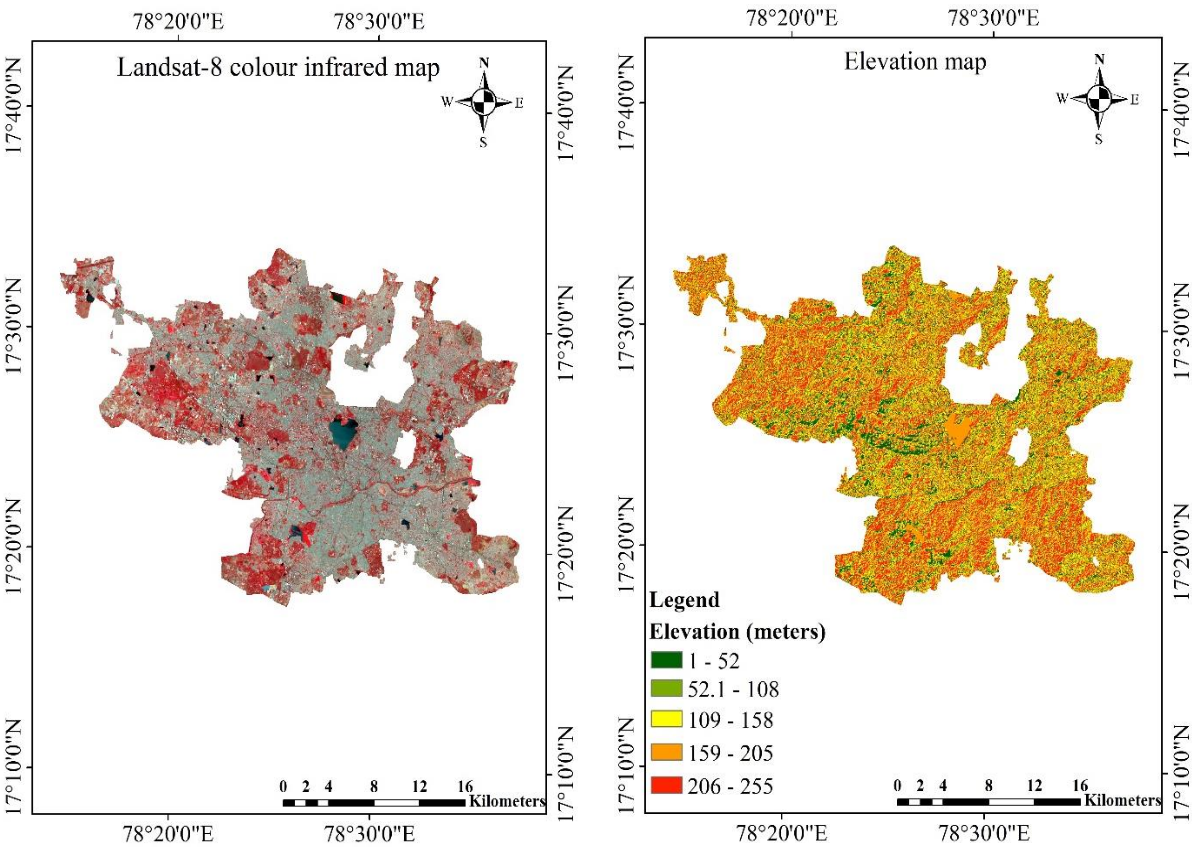

Fig. 3: Colour infrared map and elevation map of GHMC region

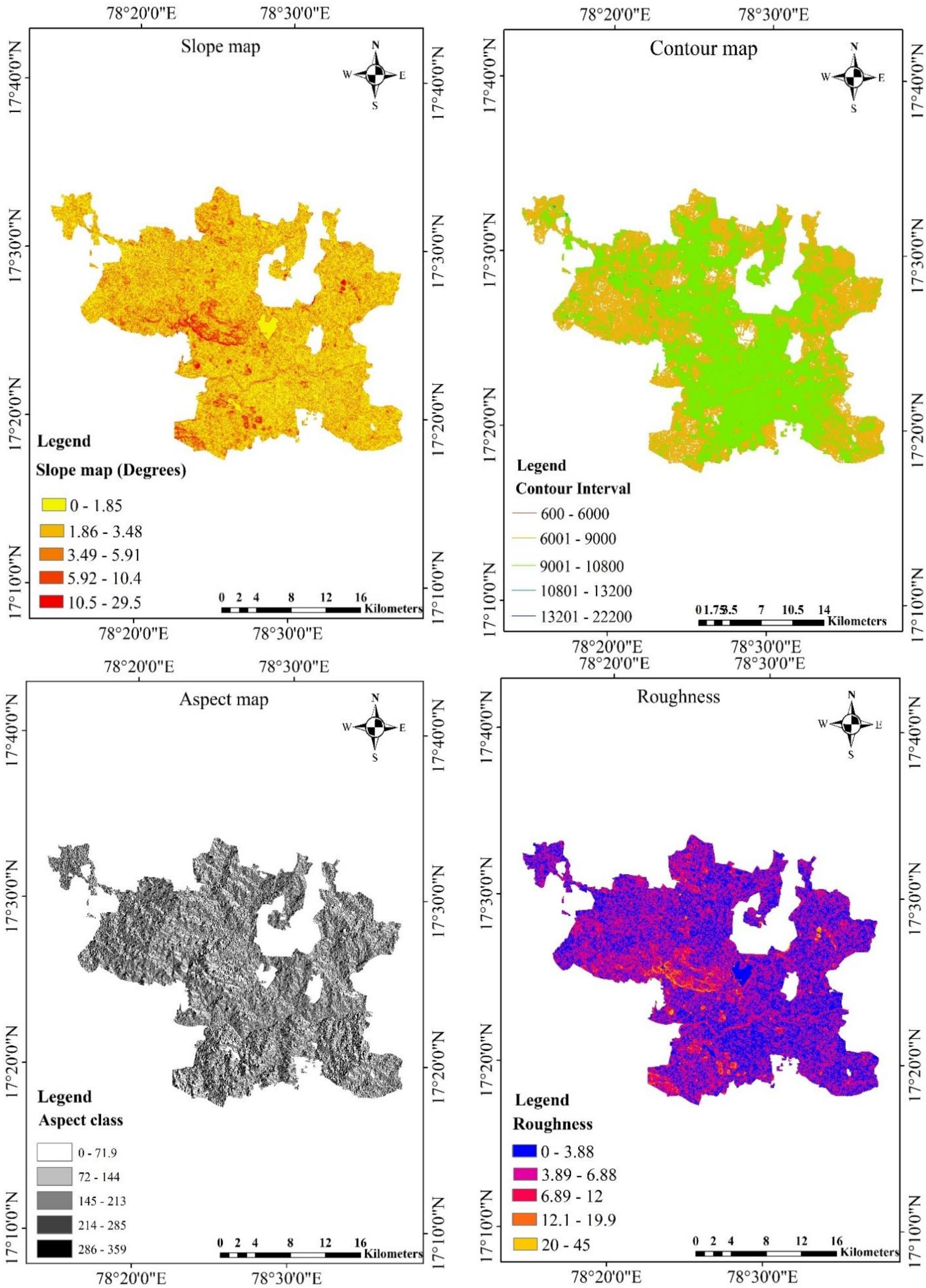

Fig. 4: Integrated slope, contour, aspect and roughness mapping of GHMC region

In this investigation focused on GHMC, the fundamental dataset for GIS analysis is established using Landsat 8 (Level-2) data sourced from the USGS website, alongside USGS-SRTM-DEM data. Employing GIS techniques like band-composting and mosaic, a colour infrared and elevation maps was generated[16] as illustrated in figure 3.

Surface characteristics: In the context of flood susceptibility mapping, understanding the terrain characteristics of a region is crucial for assessing vulnerability. Maps depicting slope, contour, roughness and aspect (Fig.4.) provide valuable insights into the topographic features that influence flood risk[22,56]. Slope maps illustrate the steepness of terrain, with lower slopes often associated with flood-prone areas due to reduced runoff. Utilizing landsat-8 data and GIS software, slope values are calculated in degrees, with a maximum slope of 29.5 degrees observed in various parts of GHMC region. Contour maps, on the other hand, delineate elevation differences, aiding in identifying low-lying regions susceptible to inundation. Roughness maps were derived through surface techniques, quantify surface irregularities, with minimum and maximum roughness values informing flood susceptibility assessments[53].

Aspect maps were categorized into directional segments, highlight the exposure of slopes to environmental factors like wind, rainfall and sunlight, influencing vegetation growth and soil moisture retention. In the context of flood susceptibility mapping, several variables play pivotal roles in assessing hydrological risks and potential flooding events[54]. Flow accumulation, for instance, serves as a key indicator, representing the total flow originating from upstream areas to a specific point within the catchment. Higher flow accumulation values signify increased water accumulation, thus elevating the likelihood of flooding. In this study, flow accumulation values are categorized into five classes, ranging from very low to very high, providing insights into flood-prone areas based on varying degrees of water accumulation potential[55]. Drainage density, another critical factor, reflects the condition of the soil and its geophysical properties, significantly impacting flood occurrences[60].

By analyzing the drainage network, the drainage density map of the study area is generated, aiding in assessing flood vulnerability and categorized into five classes, each class is assigned a rank based on its influence on flooding, ranging from areas with minimal impact to highly vulnerable zones[1]. Understanding the role of drainage density assists in delineating flood-prone regions and prioritizing mitigation efforts accordingly[62]. Heavy rainfall stands out as a primary driver of flooding events, with precipitation extremes leading to runoff and subsequent inundation[68].

Data sourced from the IMD provides crucial insights into rainfall patterns, aiding in identifying areas susceptible to flooding[59]. By categorizing cumulative rainfall of the years 2022 and 2023 amounts into high (251-1500 mm), medium (26-250 mm) and normal (0-25 mm) categories, soil types within the study region also play a significant role in regulating water infiltration and flow dynamics. With three distinct soil varieties observed, each type influences water retention and runoff differently[71]. Understanding soil characteristics aids in comprehending hydrological processes and their implications for flood risk assessment[77]. Furthermore, the distance from the drainage network serves as a crucial determinant of flood vulnerability.

Regions closer to streams experience heightened flood susceptibility, while those farther away may face lower risks[58]. By categorizing distance to the drainage network into five classes, the study delineates flood-prone zones, accordingly, aligning with research findings emphasizing the relationship between proximity to drainage networks and flood risk[75,77]. The thematic maps of flow accumulation, watershed declination (stream network), flow direction and drainage density are shown in figure 5.

LULC, NDVI and TWI mapping: Flood susceptibility mapping plays a critical role to mitigate the impact of floods in the region. Utilizing advanced techniques such as supervised image classification within a GIS, land use and land cover (LULC) maps are generated from colour infra-red imagery. Communities and uninhabited areas receive lower priority, considering their moderate ability to impede water flow[8]. In conjunction with LULC analysis, the topographic wetness index (TWI) is employed to evaluate the terrain's susceptibility to water accumulation and flow. TWI, calculated based on factors such as slope and catchment area, serves as an essential parameter in understanding soil moisture conditions and spatial variability in soil properties[3].

$$\mathrm{TWI} = \mathrm{Ln}\frac{\mathrm{a}}{\tan(\beta)} \tag{1}$$

This index aids in categorizing areas into five susceptibility classes, ranging from extremely low to high, facilitating targeted flood management strategies. Another crucial tool in flood susceptibility mapping is the Normalized Difference Vegetation Index (NDVI), which quantifies vegetation health and density by analyzing spectral reflectance. Derived from specific spectral bands, NDVI values range from -1 to 1, with higher values indicating dense vegetation and negative values indicating non-vegetated surfaces like water bodies or clouds. In this context, the NDVI is calculated using the relation shown in eq. 2 where notation B stands for band in the colour infra-red map:

$$NDVI = \frac{B5 - B4}{B5 + B4} \tag{2}$$

These maps provide detailed insights into various features of GHMC region including water bodies, urban and rural settlements, forested areas, industrial zones and natural vegetation. In prioritizing areas for flood susceptibility, particular attention is given to agricultural lands and water bodies due to their significant role in water retention. Conversely, regions inhabited by generating NDVI maps through GIS techniques, the distribution of vegetation cover across the region is assessed, aiding in flood risk evaluation. In summary, flood susceptibility mapping in the GHMC area integrates advanced GIS techniques including supervised image classification, TWI analysis and NDVI mapping. The LULC, NDVI, TWI and rainfall distributions maps are shown in figure 6.

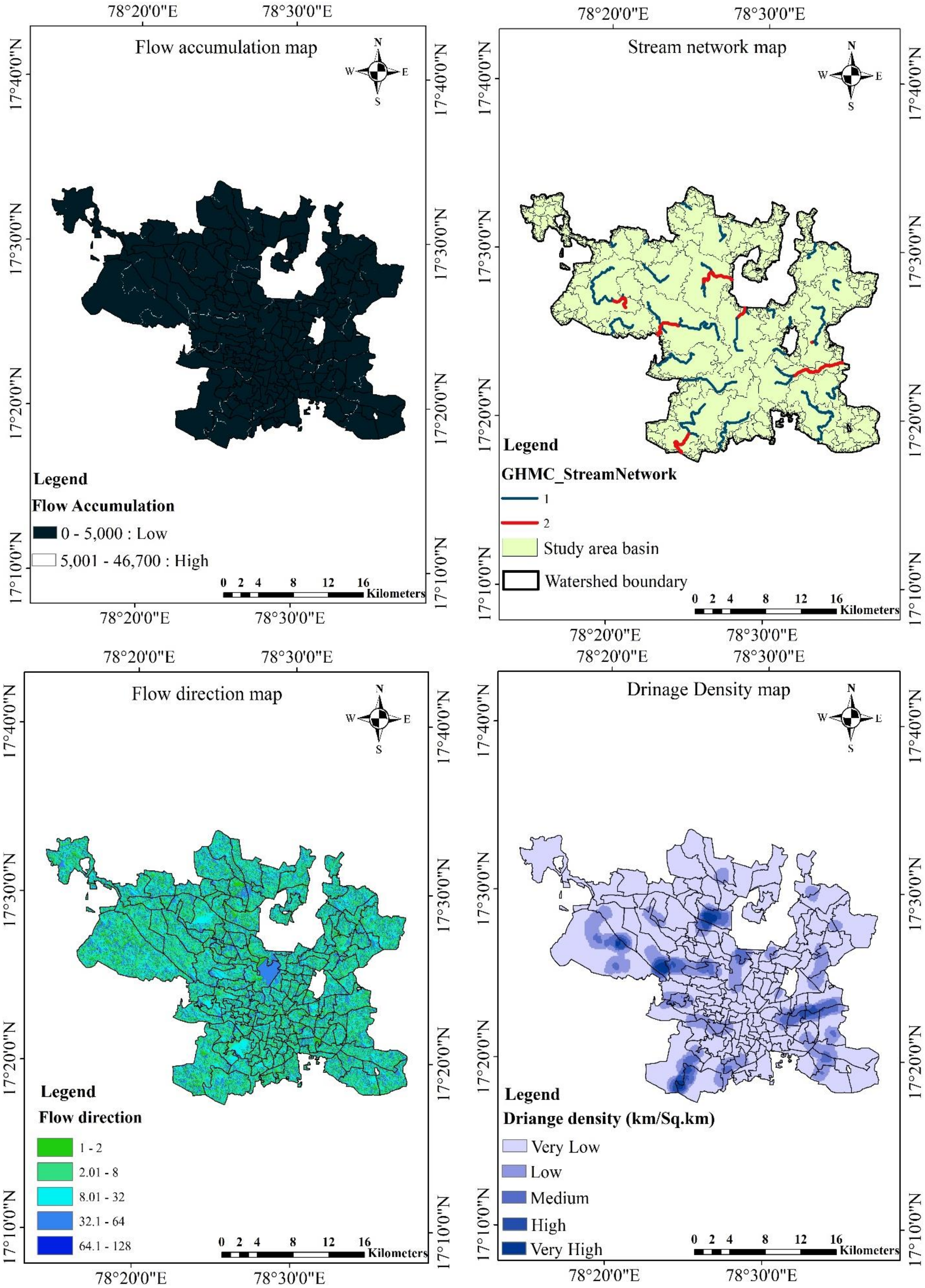

Fig. 5: Hydrological aspects of GHMC includes flow accumulation, stream network map, flow direction and drainage density map respectively.

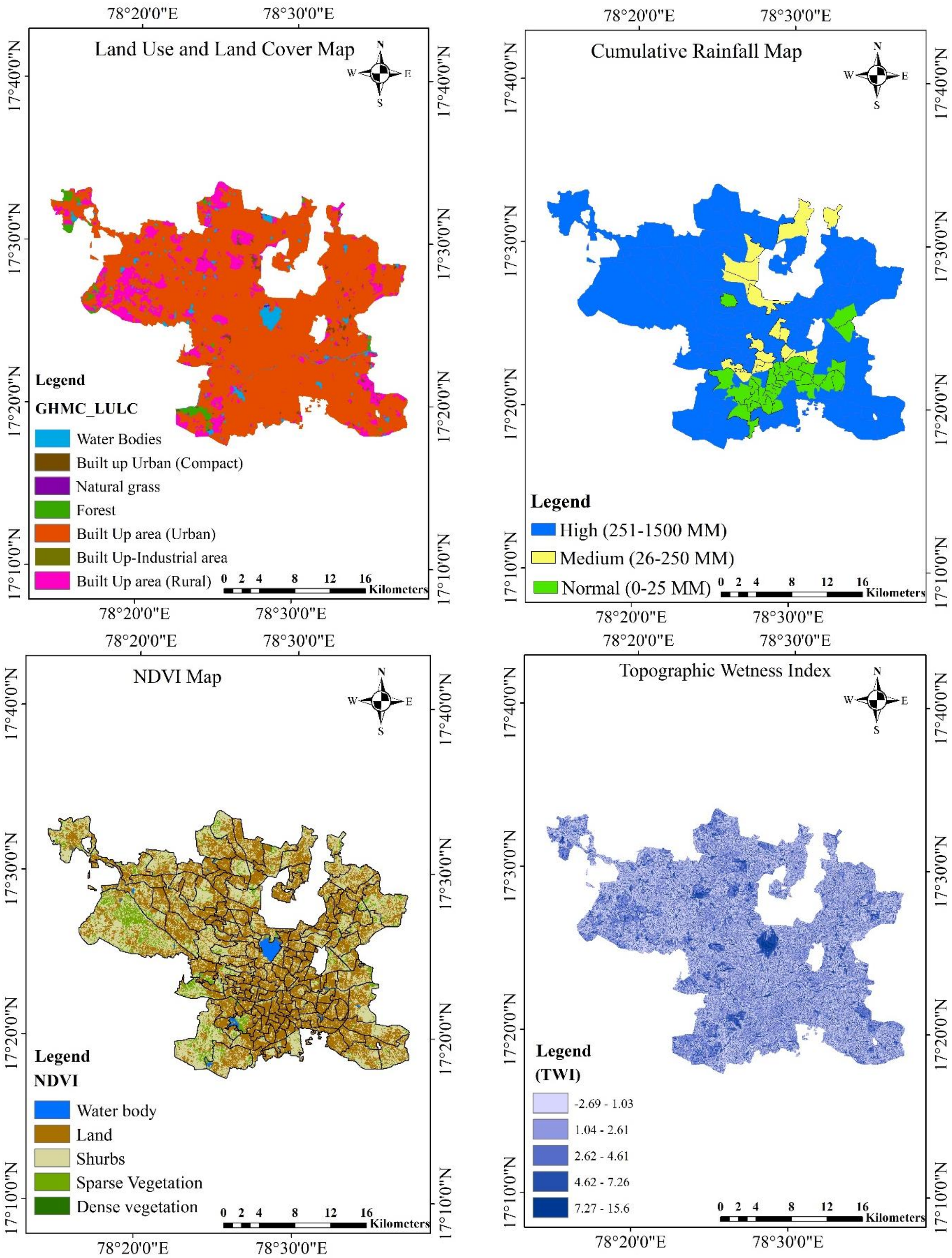

Fig. 6: LULC, Cumulative rainfall, NDVI and TWI map of GHMC region, Telangana

Implementing AHP technique and flood susceptibility mapping: Analyzing flood susceptibility and devising effective risk management strategies often entails integrating diverse spatial data layers, a task adeptly facilitated by the AHP within GIS. AHP serves as a structured decision-making tool that assigns relative weights to various map layers based on their respective influences[64]. This involves comparing the importance of different factors through pairwise comparisons, where we will assign a value indicating their relative importance[7]. These comparisons form the basis for calculating the weights of each criterion, creating a hierarchy that delineates their respective impacts on flood susceptibility.

The significance of each factor is determined by assessing the pairwise relative importance of various indicators. These criteria are organized hierarchically, with their relative significance rated on a scale from 1 to 9, indicating varying degrees of criticality[38]. The outcome of the comparison matrix for 'n' criteria can then be condensed into a summarized matrix. In this context, the weight of the criteria can be represented as a coefficient a_{ij} (i,j =1,2,3,…..n), as given in eq. 3:

$$A = \begin{bmatrix} a11 & a12 \ldots\ldots & a1n \\ a21 & a22 \ldots\ldots & a2n \\ an1 & an2 \ldots\ldots & ann \end{bmatrix}, a_{ii} = 1, a_{ij} = \frac{1}{a_{ij}}, a_{ij} \neq 0 \qquad (3)$$

Although subjectivity is inherent in the hierarchical structuring of AHP, its utilization is widely recommended for regional studies owing to its robustness[38]. The process involves multiplying the weighted values of each input raster by their corresponding cell values. To facilitate the weighted overlay analysis (WOA), all layers underwent reclassification, rasterization and resampling, ensuring uniform pixel size and labeling[40]. GIS was employed for this research, utilizing the weighted overlay technique (WOT). Ten input layers were utilized for the overlay analysis, employing the mathematical equation 4:

$$RI = \sum W_i R_j \qquad (4)$$

Here, 'W' signifies the weight assigned to each layer and 'R' denotes the rank assigned to each theme within a layer. The variable 'i' corresponds to the number of layers while 'j' corresponds to the number of themes within each layer.

$$RI = W1 \times R1 + W2 \times R2 + W3 \times R3 + W4 \times R4 + W5 \times R5 + W6 \times R6 + W7 \times R7 + W8 \times R8 + W9 \times R9 + W10 \times R10 \qquad (5)$$

where W1×R1, W2×R2 ………… W10×R10 are the weightage and ranking of TWI, elevation, slope, precipitation, LULC, NDVI, distance from river, aspect, drainage density and soil type respectively[38].

The factors were assessed based on their significance, receiving numerical ratings on a scale of 1 to 5 (Table 1). Each factor class was assigned weights and grades, with higher weights and ranks indicating a more substantial influence on flood occurrence[38,57]. Utilizing the WOM in GIS, these factors were overlaid as thematic layers to generate the flood susceptibility map[17]. The resulting risk map was categorized into three zones: low, moderate and high hazard zones as shown in figure 7.

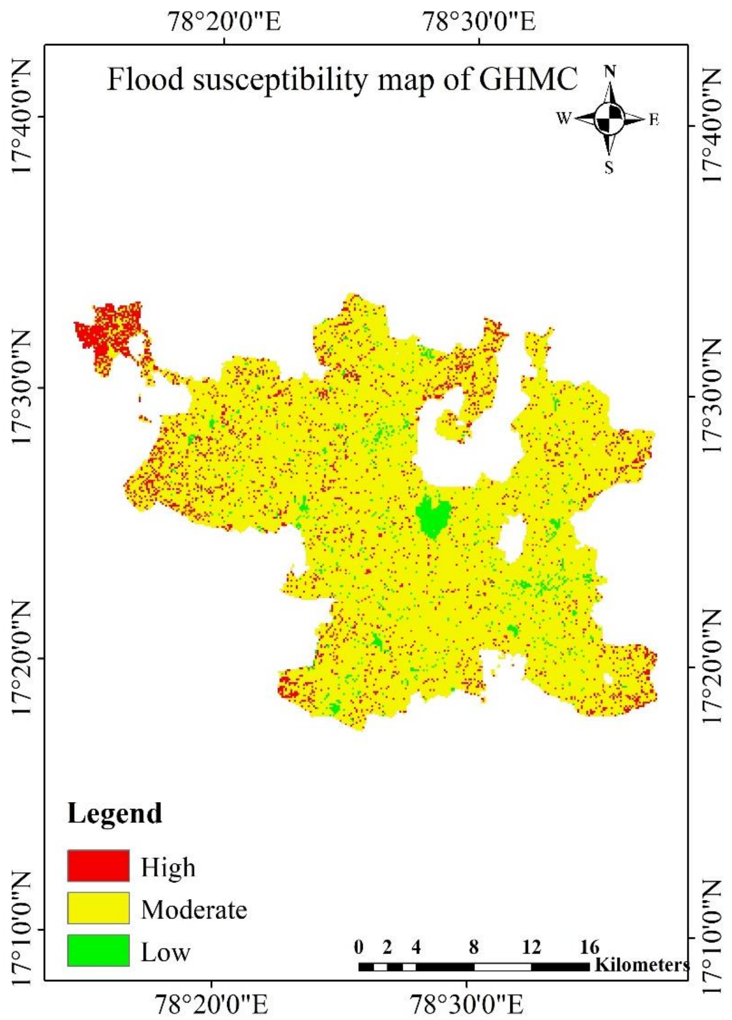

Fig. 7: Flood susceptibility map of GHMC region, Telangana

Table 1
Rank and weightages of different susceptibility classes of various thematic maps

Creation	Unit	Susceptibility class	Ratings	Weight (%)
TWI	%	Very Low	1	12
		Low	2	
		Moderate	3	
		High	4	
		Very High	5	
Elevation	Meters	Very High	5	11
		High	4	
		Moderate	3	
		Low	2	
		Very Low	1	
Slope	Degrees	Very High	5	11
		High	4	
		Moderate	3	
		Low	2	
		Very Low	1	
Precipitation	mm/year	Very Low	1	13
		Low	2	
		Moderate	3	
		High	4	
		Very High	5	
LULC	Level	Very High	5	7
		High	4	
		Moderate	3	
		Low	2	
		Very Low	1	
NDVI	Level	Very High	5	9
		High	4	
		Moderate	3	
		Low	2	
		Very Low	1	
Distance from River	Meters	Very High	5	9
		High	4	
		Moderate	3	
		Low	2	
		Very Low	1	
		Low	2	
		Moderate	3	
		High	4	
		Very High	5	
Aspect	Level	Very High	1	10
		High	2	
		Moderate	3	
		Low	4	
		Very Low	5	
Drainage density	m/km	Very Low	1	9
		Low	2	
		Moderate	3	
		High	4	
		Very High	5	
Soil type	Level	Very High	5	9
		High	4	
		Moderate	3	
		Low	2	
		Very Low	1	

Conclusion

The primary objective of this study is to conduct flood susceptibility mapping for the GHMC region. Employing a multicriteria approach, specifically GIS-AHP methodology, enabled the assignment of rankings to thematic maps. A comprehensive set of 10 thematic maps was utilized in the integration process to develop the flood susceptibility map. Initial data acquisition was accomplished from the USGS website, comprising Landsat-8 imagery, SRTM-DEM and rainfall data sourced from IMD. Spatial analytical tools within GIS were utilized for tasks such as band composition and mosaic creation, facilitating the development of essential thematic maps such as elevation, slope, aspect and roughness, offering valuable insights into surface characteristics. Furthermore, hydrological thematic maps including flow basin, flow accumulation, flow direction, drainage density, watershed declination (stream network), distance from the river and rainfall maps, were generated to comprehend flow patterns.

LULC along with TWI played pivotal roles in flood susceptibility mapping. LULC maps were categorized into five groups: water bodies, built-up areas (urban and rural), forest lands, vegetation and industrial areas. The TWI map, categorized into five classes, also contributed significantly.

The AHP emerged as the preferred approach for studying flood susceptibility, facilitating the assignment of rankings (A for highly important and B for least important) to thematic maps based on their significance. WOT was employed to assign weights and rankings to all thematic maps. Preceding the rank and weight assignment, all thematic maps were rescaled into five classes. Through the integration of these thematic maps, the flood susceptibility map for the GHMC region was meticulously crafted, categorized into low, moderate and high hazard zones. The implementation of findings from this study will be helpful to safeguard lives, properties and the overall well-being of the populace in Hyderabad, Telangana.

References

1. Aimi S.A., Andongma T.W., Ogungbade O., Senbore S.S., Alepa V.C., Akinlabi O.J., Olawale L.O. and Muhammed Q.O., Flood vulnerable zones mapping using geospatial techniques: Case study of Osogbo Metropolis, Nigeria, *The Egyptian Journal of Remote Sensing and Space Science*, **25(3)**, 841-850 **(2022)**

2. Arabameri A., Rezaei K., Cerdà A., Conoscenti C. and Kalantari Z., A comparison of statistical methods and multi-criteria decision making to map flood hazard susceptibility in Northern Iran, *Science of the Total Environment*, **660(1)**, 443-458 **(2019)**

3. Berhanu B. and Bisrat E., Identification of surface water storing sites using topographic wetness index (TWI) and normalized difference vegetation index (NDVI), *Journal of Natural Resources and Development*, **8(1)**, 91-100 **(2018)**

4. Bhukya L., Kedika N.R. and Salkuti S.R., Enhanced maximum power point techniques for solar photovoltaic system under uniform insolation and partial shading conditions: a review, *Algorithms*, **15(10)**, 365 **(2022)**

5. Bhukya M.N. and Kota V.R., A quick and effective MPPT scheme for solar power generation during dynamic weather and partial shaded conditions, *Engineering Science and Technology, An International Journal*, **22(3)**, 869-884 **(2019)**

6. Cai S., Fan J. and Yang W., Flooding risk assessment and analysis based on GIS and the TFN-AHP method: a case study of Chongqing, China, *Atmosphere*, **12(5)**, 623-648 **(2021)**

7. Chakraborty S. and Mukhopadhyay S., Assessing flood risk using analytical hierarchy process (AHP) and geographical information system (GIS): application in Coochbehar district of West Bengal, India, *Natural Hazards*, **99(1)**, 247-274 **(2019)**

8. Chandra M.K. and Aitch Pritam S.S., Flood hazards and risk prediction by using the Analytical Hierarchy Process on GIS platform: a case study in lower Ajay basin, India, *Disaster Advances*, **16(1)**, 1-13 **(2023)**

9. Chandramouli C. and General R., Census of India, Rural urban distribution of population, provisional population total, New Delhi, Office of the Registrar General and Census Commissioner, India **(2011)**

10. Chang K.T. and Tsai B.W., The effect of DEM resolution on slope and aspect mapping, *Cartography and Geographic Information Systems*, **18(1)**, 69-77 **(1991)**

11. Chanu M.L. and Bakimchandra O., Landslide susceptibility assessment using AHP model and multi resolution DEMs along a highway in Manipur, India, *Environmental Earth Sciences*, **81(5)**, 156 **(2022)**

12. Chen H., Ito Y., Sawamukai M. and Tokunaga T., Flood hazard assessment in the kujukuri plain of chiba prefecture, japan, based on GIS and multicriteria decision analysis, *Nat Hazards*, **78(1)**, 105–120 **(2015a)**

13. Cheruvu A., Radhakrishna V. and Rajasekhar N., Using normal distribution to retrieve temporal associations by Euclidean distance, In 2017 International Conference on Engineering & MIS (ICEMIS), IEEE, 1-3 **(2017)**

14. Danumah J.H., Odai S.N., Saley B.M., Szarzynski J., Thiel M., Kwaku A., Kouame F.K. and Akpa L.Y., Flood Risk Assessment and Mapping in Abidjan District Using Multi-Criteria Analysis (AHP) Model and Geoinformation Techniques, (Cote d'ivoire), *Geoenvironmental Disasters*, **3(10)**, 1-13 **(2016)**

15. Devi M.D., Juliet A.V., Hariprasad K., Ganesh V., Ali H.E., Algarni H. and Yahia I.S., Improved UV Photodetection of Terbium-doped NiO thin films prepared by cost-effective nebulizer spray technique, *Materials Science in Semiconductor Processing*, **127**, 105673 **(2021)**

16. El-Quilish M., El-Ashquer M., Dawod G. and El Fiky G., Development and accuracy assessment of high-resolution digital elevation model using GIS approaches for the Nile Delta Region, Egypt, *American Journal of Geographic Information System*, **7(4)**, 107-117 **(2018)**

17. Elsheikh R.F.A., Ouerghi S. and Elhag A.R., Flood risk map based on gis and multi criteria techniques (case study terengganu malaysia), *J Geogr Inf Syst*, **7(04)**, 348–357 **(2015)**

18. Flood toll 32 and counting in Telangana, The New Indian Express, Archived from the original on 21 October 2020, Retrieved 20 October 2023 **(2020)**

19. Floods in Telangana claim 50 lives, state suffers Rs 5,000 crore damages, Deccan Herald, 15 October 2020, Archived from the original on 21 October 2020, Retrieved 20 October 2023 **(2020)**

20. Gade M.S.L. and Rooban S., Run time fault tolerant mechanism for transient and hardware faults in alu for highly reliable embedded processor, In 2020 International Conference on Smart Technologies in Computing, Electrical and Electronics (ICSTCEE), 44-49 **(2020)**

21. Goud B.S., Srilatha P. and Shekar M.R., Effects of mass suction on MHD boundary layer flow and heat transfer over a porous shrinking sheet with heat source/sink, *Int. Journal of Innovative Technology and Exp. Engineering*, **8(10)**, 263-266 **(2019)**

22. Grohmann C.H., Smith M.J. and Riccomini C., Multiscale analysis of topographic surface roughness in the Midland Valley, Scotland, *IEEE Transactions on geoscience and Remote Sensing*, **49(4)**, 1200-1213 **(2010)**

23. Gupta S.K. and Shukla D.P., Evaluation of topographic correction methods for LULC preparation based on multi-source DEMs and Landsat-8 imagery, *Spatial Information Research*, **28(1)**, 113-127 **(2020)**

24. Ihse M., Colour infrared aerial photography as a tool for vegetation mapping and change detection in environmental studies of Nordic ecosystems: A review, *Norwegian Journal of Geography*, **61(4)**, 170-191 **(2007)**

25. Jagadha S., Gopal D. and Kishan N., Nanofluid flow of higher order radiative chemical reaction with effects of melting and viscous dissipation, *Journal of Physics*, Conference Series, IOP Publishing, **1451(1)**, 012003, **(2020)**.

26. Jose S. et al, Characterisation of absorbing aerosols using ground and satellite data at an urban location, Hyderabad, *Aerosol and Air Quality Research*, **16(6)**, 1427-1440 **(2016)**

27. Kalyani G., Janakiramaiah B., Karuna A. and Prasad L.N., Diabetic retinopathy detection and classification using capsule networks, *Complex & Intelligent Systems*, **9(3)**, 2651-2664 **(2023)**

28. Kalyani G., Janakiramaiah B., Prasad L.N., Karuna A. and Babu A.M., Efficient crowd counting model using feature pyramid network and ResNeXt, *Soft Computing*, **25(15)**, 10497-10507 **(2021)**

29. Khosravi K., Shahabi H., Pham B.T., Adamowski J., Shirzadi A., Pradhan B., Dou J., Ly H.B., Gróf G., Ho H.L. and Hong H., A comparative assessment of flood susceptibility modeling using multi-criteria decision-making analysis and machine learning methods, *Journal of Hydrology*, **573**, 311-323 **(2019)**

30. Kotecha M.J., Tripathi G., Singh S.K., Kanga S., Meraj G., Sajan B. and Rai P.K., GIS-Based novel ensemble MCDM-AHP modeling for flash flood susceptibility mapping of Luni River Basin, Rajasthan, In River Conservation and Water Resource Management, Singapore, Springer Nature Singapore, **14**, 267-313 **(2023)**

31. Kumar C.L., Jayakumar V. and Bharathiraja G., Optimization of welding parameters for friction stir spot welding of AA6062 with similar and dissimilar thicknesses, Materials Today: Proceedings, **19**, 251-255 **(2019)**

32. Kumar K.U., Babu P., Basavapoornima C., Praveena R., Rani D.S. and Jayasankar C.K., Spectroscopic properties of Nd3+-doped boro-bismuth glasses for laser applications, *Physica B: Condensed Matter*, **646(1)**, 414327 **(2022)**

33. Kumar N.R., Goud S.J., Srilatha P., Manjunatha P.T., Rani S.P., Kumar R. and Suresha S., Cattaneo–Christov heat flux model for nanofluid flow over a curved stretching sheet: An application of Stefan blowing, *Heat Transfer*, **51(6)**, 4977-4991 **(2022)**

34. Kumar S., Reddy M.M., Meena I. and Vijay K.A., Monitoring and Assessment of Drought using Remote Sensing and association rules, *Disaster Advances*, **16(10)**, 30-40 **(2023)**

35. Kumar S., Reddy M.M., Meena I., Kumar S.M., Flood frequency and flood forecasting analysis of Krishna basin Andhra Pradesh, *Disaster Advances*, **16(11)**, 27-39 **(2023)**

36. Kumari C.U. et al, An automated detection of heart arrhythmias using machine learning technique: SVM, Materials Today: Proceedings, **45(1)**, 1393-1398 **(2021)**

37. Lakshmi L., Reddy M.P., Santhaiah C. and Reddy U.J., Smart phishing detection in web pages using supervised deep learning classification and optimization technique ADAM, *Wireless Personal Communications*, **118(4)**, 3549-3564 **(2021)**

38. Lin L., Wu Z. and Liang Q., Urban flood susceptibility analysis using a GIS-based multi-criteria analysis framework, *Natural Hazards*, **97(2)**, 455-475 **(2019)**

39. Liuzzo L., Sammartano V. and Freni G., Comparison between different distributed methods for flood susceptibility mapping, *Water Resources Management*, **33(9)**, 3155-3173 **(2019)**

40. Malczewski J., GIS-based multicriteria decision analysis: a survey of the literature, *Int. J Geogr. Inf Sci*, **20(7)**, 703–726 **(2006)**

41. Malliga S. et al, Hyperparameter Optimization for Transfer Learning of VGG16 for Disease Identification in Corn Leaves Using Bayesian Optimization, *Big Data*, **10(3)**, 215-229 **(2022)**

42. Mandapudi S., Chaganti S.S., Gorle S., Prasad S.U., Govardhan D. and Praveen B., CFD simulation of flow past wing body junction: a 3-D approach, *International Journal of Mechanical and Production Engineering Research and Development*, **7(4)**, 341-350 **(2017)**

43. Mohammed A. and Regonda S.K., Synoptic circulation patterns of urban floods for the city of Hyderabad, *International Journal of Climatology*, **43(15)**, 7032-7049 **(2023)**

44. Mudashiru R.B., Sabtu N. and Abustan I., Quantitative and semi-quantitative methods in flood hazard/susceptibility mapping: a review, *Arabian Journal of Geosciences*, **14(11)**, 941 **(2021)**

45. Nagarjuna T., Lakshmi S. and Nehru K., USRP 2901-based SISO-GFDM transceiver design experiment in virtual and remote laboratory, *The International Journal of Electrical Engineering and Education*, **59(4)**, 350-365 **(2022)**

46. Ouma Y. and Tateishi R., Urban food vulnerability and risk mapping using integrated multi-parametric AHP and GIS: methodological overview and case study assessment, *Water*, **6(6)**, 1515–1545 **(2014)**

47. Padmaja B., Myneni M.B. and Krishna Rao Patro E., A comparison on visual prediction models for MAMO (multi activity-multi object) recognition using deep learning, *Journal of Big Data*, **7(1)**, 1-15 **(2020)**

48. Padmaja B., Prasad V.R. and Sunitha K.V.N., A machine learning approach for stress detection using a wireless physical activity tracker, *International Journal of Machine Learning and Computing*, **8(1)**, 33-38 **(2018)**

49. Pham B.T., Jaafari A., Van Phong T., Yen H.P.H., Tuyen T.T., Van Luong V., Nguyen H.D., Van Le H. and Foong L.K., Improved flood susceptibility mapping using a best first decision tree integrated with ensemble learning techniques, *Geoscience Frontiers*, **12(3)**, 101-105 **(2021)**

50. Pon V.D., Wilson K.J., Hariprasad K., Ganesh V., Ali H.E., Algarni H. and Yahia I.S., Enhancement of optoelectronic properties of ZnO thin films by Al doping for photodetector applications, *Superlattices and Microstructures*, **151(1)**, 106790 **(2021)**

51. Radhakrishna V., Kumar P.V., Janaki V. and Rajasekhar N., Estimating prevalence bounds of temporal association patterns to discover temporally similar patterns, *Advances in Intelligent Systems and Computing*, **576(2)**, 209-220 **(2017)**

52. Raji A. et al, Biowaste-originated heteroatom-doped porous carbonaceous material for electrochemical energy storage application, *Journal of Industrial and Engineering Chemistry*, **98(1)**, 308-317 **(2021)**

53. Ramu G., A secure cloud framework to share EHRs using modified CP-ABE and the attribute bloom filter, *Education and Information Technologies*, **23(5)**, 2213-2233 **(2018)**

54. Reddy M.M., Rani S.P., Naresh N., Sai Kumar R. and Janaki V., Assessing flood susceptibility in the Godavari River Basin, Bhadrachalam Region, Sothern India: A GIS-AHP Multi-Criteria Approach, *Disaster Advances*, **17(5)**, 61-71 **(2024)**

55. Rizwana M.S. and Sarah P., Impedance and electromechancial studies on Ca0. 1Sr0. 9LaxBi2-xTa2O9 ceramics, *Ferroelectrics*, **524(1)**, 95-101 **(2018)**

56. Rowbotham D.N. and Dudycha D., GIS modelling of slope stability in Phewa Tal watershed, Nepal, *Geomorphology*, **26(1-3)**, 151-170 **(1998)**

57. Saaty T.L., Decision making with the analytic hierarchy process, *Int J Serv Sci*, **1(1)**, 83–98 **(2008)**

58. Saghafian B., Regional hydrologic mapping of flows in stream networks, *International Journal of Applied Earth Observation and Geoinformation*, **11(5)**, 317-323 **(2009)**

59. Saicharan V. and Rangaswamy S.H., A Comparison and Ranking Study of Monthly Average Rainfall Datasets with IMD Gridded Data in India, *Sustainability*, **15(7)**, 5758 **(2023)**

60. Sastry Y.S., Budarapu P.R., Krishna Y. and Devaraj S., Studies on ballistic impact of the composite panels, *Theoretical and Applied Fracture Mechanics*, **72(1)**, 2-12 **(2014)**

61. Seydi S.T., Kanani-Sadat Y., Hasanlou M., Sahraei R., Chanussot J. and Amani M., Comparison of machine learning algorithms for flood susceptibility mapping, *Remote Sensing*, **15(1)**, 192 **(2022)**

62. Shejkar S.K., Agrawal B., Agrawal A., Gupta G. and Pati P.R., Influence of filler content and surface modification on physical and mechanical properties of epoxy/walnut shell particulate composites, *Journal of Adhesion Science and Technology*, **37(7)**, 1215-1232 **(2023)**

63. Siart C., Bubenzer O. and Eitel B., Combining digital elevation data (SRTM/ASTER), high resolution satellite imagery (Quickbird) and GIS for geomorphological mapping: A multi-component case study on Mediterranean karst in Central Crete, *Geomorphology*, **112(1-2)**, 106-121 **(2009)**

64. Souissi D., Zouhri L., Hammami S., Msaddek M.H., Zghibi A. and Dlala M., GIS-based MCDM–AHP modeling for flood susceptibility mapping of arid areas, southeastern Tunisia, *Geocarto International*, **35(9)**, 991-1017 **(2020)**

65. Spandana K. and Rao V.S., Internet of things (Iot) based smart water quality monitoring system, *International Journal of Engineering & Technology*, **7(3)**, 259-262 **(2018)**

66. Special Tropical Weather Outlook, RSMC New Delhi, 11 October 2020, Archived from the original on 18 October 2020, Retrieved 18 October 2023 **(2020)**

67. Swain K.C., Singha C. and Nayak L., Flood susceptibility mapping through the GIS-AHP technique using the cloud, *ISPRS International Journal of Geo-Information*, **9(12)**, 720 **(2020)**

68. Telagam N., Kandasamy N. and Nanjundan M., Smart sensor network based high quality air pollution monitoring system using labview, *International Journal of Online Engineering*, **13(08)**, 79-87 **(2017)**

69. Tucker G.E., Catani F., Rinaldo A. and Bras R.L., Statistical analysis of drainage density from digital terrain data, *Geomorphology*, **36(3-4)**, 187-202 **(2001)**

70. Vadlamudi Swathi, Rain fury leaves capital battered, bruised, *The Hindu*, Archived from the original on 15 October 2020, Retrieved 15 October 2023 **(2020)**

71. Vallabhuni R.R., Lakshmanachari S., Avanthi G. and Vijay V., Smart cart shopping system with an RFID interface for human assistance, In 2020 3rd International Conference on Intelligent Sustainable Systems (ICISS), IEEE, 165-169 **(2020)**

72. Vemula S., Raju K.S., Veena S.S. and Kumar A.S., Urban floods in Hyderabad, India, under present and future rainfall scenarios: a case study, *Natural Hazards*, **95(1)**, 637-655 **(2019)**

73. Vemula V.A., Bhatt C.M. and Umamahesh N.V., Rapid assessment of the October 2020 Hyderabad urban flood and risk analysis using geospatial data, *Current Science*, **120(12)**, 1840-1847 **(2021)**

74. Vilasan R.T. and Kapse V.S., Evaluation of the prediction capability of AHP and F-AHP methods in flood susceptibility mapping of Ernakulam district (India), *Natural Hazards*, **112(2)**, 1767-1793 **(2022)**

75. Yilmaz O.S., Flood hazard susceptibility areas mapping using Analytical Hierarchical Process (AHP), Frequency Ratio (FR) and AHP-FR ensemble based on Geographic Information Systems (GIS): a case study for Kastamonu, Türkiye, *Acta Geophysica*, **70(6)**, 2747-2769 **(2022)**

76. Yue L., Jayapal M., Cheng X., Zhang T., Chen J., Ma X., Dai X., Lu H., Guan R. and Zhang W., Highly dispersed ultra-small nano Sn-SnSb nanoparticles anchored on N-doped graphene sheets as high-performance anode for sodium ion batteries, *Applied Surface Science*, **512(1)**, 145686 **(2020)**

77. Zhang H., Loáiciga H.A., Feng L., He J. and Du Q., Setting the Flow Accumulation Threshold Based on Environmental and Morphologic Features to Extract River Networks from Digital Elevation Models, *ISPRS International Journal of Geo-Information*, **10(3)**, 186-211 **(2021)**.

(Received 02nd March 2024, accepted 06th May 2024)